AOTF Polarimetric Hyperspectral Imaging for Mine Detection

Li-Jen Cheng and George Reyes
Jet Propulsion Laboratory
California Institute of Technology
Pasadena, CA 91109

ABSTRACT

This paper reports an analysis of polarimetric hyperspectral imagery of an outdoor scene containing a number of inactive mines. The imagery was taken with a visible/near-infrared acousto-optic tunable filter prototype system. The result has illustrated that the characteristics of mine smooth surfaces can create high signals in polarization difference images and consequently provide a quick and reliable approach for detection.

1. INTRODUCTION

Polarimetric hyperspectral imaging (PHI) is an effective remote sensing technique, because it takes imagery of a scene as a function of wavelength and polarization. This side-by-side comparison of the spectral and polarization signatures in the image format is a powerful way to detect targets in cluttered environments.

Using a visible/near-infrared acousto-optic tunable filter (AOTF) PHI prototype system operating in a wavelength range of 0.48-0.75 microns[1], we did a number of outdoor field experiments to evaluate the technology capability in remote sensing for observations of natural and man-made objects.[2,3,4] The experiments have illustrated that the system can classify and map natural and resource objects, such as those related to vegetation, minerals, and atmosphere. Furthermore, the system can provide an excellent target discrimination capability so that it can remotely detect targets of interest in a camouflaged or cluttered environment.

This paper reports results from an analysis of a set of AOTF-PHI observation data with the objective to detect inactive mines in a cluttered environment. The results illustrate a potential quick and reliable approach to detect mines. The observation experiment condition and some data were reported previously[4].

Mines and mine-like targets are commonly small-size objects in the dimension of 30-40 cm. When they are placed in outdoor environment, light scattering and reflection properties of the surrounding will affect observable spectra of the target. This is due to that the measured spectrum of the target is a weighted sum of its own spectrum and those of the surrounding objects. This phenomenon is known as spectral mixing, that was discussed previously.[4] The problem is expected to become more serious for smaller targets, especially for those partially buried in the surrounding.

Polarization is a complicated observable parameter because of two physical phenomena. The first is that the incident sunlight onto the scene is usually polarized due to sun light scattering at molecules and aerosols in the atmosphere, The second is that the scattering and reflection of incident light at the target surface do often alter light polarization, because the surfaces are generally made of dielectric materials. The polarization change depends not only on incident angle of the light upon the surface, but also on surface material, surface geometry, and surface textures. Consequently, the combination of polarization and spectral measurements in image format can provide needed discrimination capabilities for target detection, even in the condition that spectral mixing in the observation is substantial. The main distinguishing feature is due to the fact that the mine has smooth painted surfaces whose reflection properties are significantly different from those of natural objects, such as grass and leaves, and other man-made objects, such as cement blocks anti plastic objects. This difference provides distinguishable polarization spectral signatures.

2. OBSERVATION CONDITION

Figure 1 gives a grayscale image of an iceplant field scene with a group of targets of intc.rest whose locations were indicated in a sketch at the right. The targets included seven inactive mines: one green square plastic (D), two green round metallic (A and C), two dark green round metallic (G and H), and three dark brown round metallic (1 and J). Some mines were place.(1 on the top of the iceplant and some were pushed into the iceplant field so that only a portion of the target was visible. in addition, there were two partially observable cement blocks (B and E) , and one buried white plastic pipe with one foot length being observable (1 '). The iceplant field was a mixture of healthy and dead iceplants with uneven distribution. in addition, portions of healthy iceplants were in blossom with orange flowers. This arrangement did provide an interesting challenge for testing the system.

The right upper comer of the scene were a pile of metallic sheets and parts whose images were removed during the data analysis so that we can obtain a better dynamic range in the area of interest. Two 1 Ialon plates (K and 1.) of Lambertian surface reflectance over the instrument wavelength range were also placed in the scene for intensity normalization among different wavelengths.

The P] 11 system was on the top of a small hill and looked at tile area with a downward angle of about 30 degrees and directed at 210 degrees SOL](11. The observation was carried out at the noon. The iceplant field was located about 40 meter away from the system and on a small plateau of the hill. The weather was sunny with typical Los Angles basin smog in June.

3. SPECTRAL IMAGES WIT]] TW() D IFFERENT POLARIZATION 1)1 RECTIONS

Figures 2 and 3 give two sets of six spectral images with H and V polarizations, respectively, which illustrate several interesting observations as the follow:

1[is well-known that the green vegetation in the near infrared range, such as 0.75 micron, is highly reflective, because the wavelength is beyond that of the chlorophyll absorption red edge. 1 Iowever, the reflectivity often varies with vegetation type. In the images of 0.75 microns, all bright areas were green plants, such as iceplants and some unknown green groun(i-cover plants, 111 the upper pall of images, there was a dark ci rcul ar dot surrounded by a very bright area, The dark dot was a green round metal i ic

mine (A), surrounded by a mixer of iceplants and unknown green ground-cover plants. The latter has high reflectivity in the near infrared range. Another mine, C, also appeared as a dark spot surrounded with healthy iceplants. Actually, all mines appeared to be darker in the image related to iceplants, because none of these mines had good camouflage paints that could mimic vegetation spectra well in the near infrared range.

2. We have observed that the targets in the images of V polarization were more brighter than those in the images of H polarization. This observation illustrated the existence of polarization dependence. For example, each of the green round metallic mines (A and C) appeared to have a very bright spot in the all visible wavelengths at V polarization, whereas the same mine had only a moderate reflection signal at H polarization. The bright dot appearance of mines (A and C) was due to direct plane reflection at the mine surfaces. Similarly, the green square plastic mine (D) was aiso brighter in the V polarization. This polarization difference is an important phenomenon that will be used to distinguish mines from other objects (to be discussed in the next section).

3. We noted that the intensities of the images for V polarization were always higher than those for H polarization, indicating that the incident light was partially polarized favorably toward the V polarization.

4. The iceplant flowers showed up as weak bright spots in spectral images of both polarizations at 0.55, 0.58, and 0.63 microns. The blossoming iceplants were mainly located in lilt areas of lower right and upper left parts of the scene.

5. Cement blocks and white plastic pipe were bright objects in both H and V polarizations in the visible wavelengths.

6. In the near infrared image, there was an irregular shape dark area between mines C and G, that is due to dead iceplants, because dead vegetation was relatively absorptive in the near infrared. However, it became brighter objects at red wavelength range, whereas live iceplants were very absorptive due to chlorophyll.

7. We noted that the Halon plate (K) in the image of 0.75 micron was not bright as some vegetation, illustrating the angular dependence of the Lambertian surface reflection. However, the plate was the brightest object in the images of all other wavelengths.

4.1'01 ARIZATION DIFFERENCE IMAGES AT DIFFERENT WAVELENGTHS

Figure 3 is a set of six polarization difference images formed from the spectral images of Figures 1 and 2 using the formula of polarization difference $\Delta P=(I_v - I_h)/(I_v + I_h)$, where I_v and I_h are intensities of vertically and horizontally polarized light at each pixel. The significant observation from these polarization difference images is that all the seven mines appeared to be bright spots in the green wavelength range, whereas the white plastic pipe and the cement blocks became dark and difficult to be observed. This observation has illustrated the advantage of using P]] i to detect targets of interest in a cluttered environment. The observation can be attributed to the fact that the mines have smooth painted surfaces.

We noted that the cement block, 1 C, had a bright spot its upper right corner at the wavelengths of 0.58, 0.63, 0.69 microns, presumably due to direct plane reflection. Also, we noted that the upper right edge of the plastic mine, D, had a similar bright line. Both bright reflection features disappeared in the polarization difference images at 0.52 and 0.55 microns. This disappearance was presumably due to spectral dependence of the plane reflection at the corner of the cement block and the edge of the plastic mine. However, we do not understand the phenomenon at this moment.

The spectral images in Figures 2 and 3 have shown that man-made objects, including white plastic pipe, cement blocks, as well as some of mines, had higher light reflection signals and appeared to be bright objects, but not all mines had the same reflection signals. This illustrates that spectral images are not adequate for mine detection.

It is very important to point out that all the mines had high polarization difference signals in comparison with all the other objects in the scene. The presentation of PDI data in polarization difference format seems to provide a classification of targets with smooth surfaces from those without. This classification was done without any detailed study of spectral properties. Consequently, the result indicates that polarization difference imaging is useful for target detection. TWIR systems with a limited data processing capability can provide polarization difference images in real time.

5. CONCLUSION

We performed data analysis of a field observation of mines in a cluttered environment using an AOTF PDI system. The results have illustrated that all mines in the scene had higher polarization difference signals in green wavelengths than other man-made objects and natural background. This classification using polarization difference in the image format is a valuable tool for detection of targets with smooth painted surfaces.

6. ACKNOWLEDGMENT

We would like to acknowledge the contribution of Dr. E. R. Suiter, Coastal Systems Station, Naval Surface Warfare Center, Dahlgern Division, for his directorship in the field observation experiments.

The research described in this paper was performed by the Center for Space Microelectronics Technology, Jet Propulsion Laboratory, California Institute of Technology, and was jointly sponsored by the Marine Corps Systems Command, Code AW, and National Aeronautics and Space Administration, Office Of Advanced Concepts and Technology.

7. REFERENCES

1. Li-Jen Cheng, Tien-Hsin Chao, Mack Dowdy, Clayton LaBar, Colin Mahoney, George Reyes, and Ken Bergman, "Multispectral imaging Systems Using Acousto-Optic Tunable Filter", in "Infrared and Millimeter Wave Engineering", SPIE Proceedings, Vol. 1874, p. 224 (1993).

2. L.J. Cheng, M.K. Hamilton, J.C. Mahoney, G. F. Reyes, "Analysis of AOTF 1 lyperspectral Imagery", in "Algorithms for Multi spectral and I 1 yperspectral Imagery", SPIE Proceedings, Vol. 223], p158-166 (1994).
3. Li-Jen Cheng, "A Polarimetric Hyperspectral imaging Sens, To published in the proceedings of the International Conference on Applications of Photonic Technology, June 2 I -23, 1994, Toronto, Ontario, Canada.

4. 1.. J. Cheng, J.C. Mahoney, G.F. Reyes, and H.R. Suiter, "Target Detection Using an AOTF Hyperspectral Imager", in "Optical Pattern Recognition V", SPIE Proceedings, Vol. 2237, p.25 1-259 (1994).

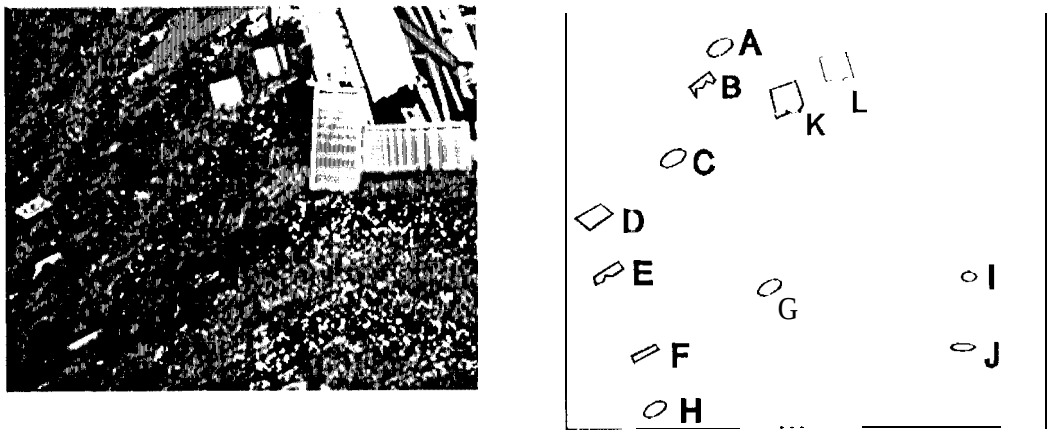

Figure 1 **Left:** **Image of the iceplant field taken** using an ordinary 35 mm camera.
Right: Sketch for locations of objects of interest in the iceplant field.
Dark green round metallic mines (A and C), a green square plastic mine (d),
dark green round metallic mines (G and H), dark brown round metallic reifies (1 and J),
cement blocks (B and E), white plastic pipe (F), and halon plates (K and L).